Analysis of parasitic cyan luminescence occurring in GaInN blue light-emitting diodes

Qifeng Shan,[1,a)] Yong Suk Cho,[2] Guan-Bo Lin,[2] David S. Meyaard,[2] Jaehee Cho,[2] E. Fred Schubert,[1,2] Joong Kon Son,[3] and Cheolsoo Sone[3]
[1]*Future Chips Constellation, Department of Physics, Applied Physics and Astronomy, Rensselaer Polytechnic Institute, Troy, New York 12180, USA*
[2]*Department of Electrical, Computer, and Systems Engineering, Rensselaer Polytechnic Institute, Troy, New York 12180, USA*
[3]*Advanced Development Group, LED Business, Samsung Electronics, Yongin 446-920, Korea*

(Received 23 April 2012; accepted 29 August 2012; published online 9 October 2012)

GaInN blue light-emitting diodes (LEDs) emitting at 445 nm exhibit a spatially uniform cyan emission (480 nm) that dominates the emission spectrum at low injection current. Photoluminescence using resonant optical excitation shows that the cyan emission originates from the active region. The blue-to-cyan intensity ratio, which depends on the electrical and optical excitation density, reveals that the cyan emission is due to a transition from the conduction band to a Mg acceptor having diffused into the last-grown quantum well of the active region. The Mg in the active region provides an additional carrier-transport path, and therefore can explain the high subthreshold forward leakage current that is measured in these LEDs. © *2012 American Institute of Physics*. [http://dx.doi.org/10.1063/1.4754829]

I. INTRODUCTION

Due to their very high efficiency and long lifetime, GaInN blue light-emitting diodes (LEDs) are used in an increasing number of applications, including general lighting applications and display-backlighting applications. However, GaInN blue LEDs can still suffer from non-ideal characteristics, such as a large reverse leakage current,[1,2] a large subthreshold forward leakage current,[3] and undesired parasitic emission bands having peak wavelengths longer than the blue band-edge emission.[4–7] For example, Leung *et al.* found an emission at 540 nm in blue LEDs emitting at 440 nm.[6] The undesired parasitic long-wavelength emission bands found in GaInN LEDs have been attributed to the tunneling-assisted radiative recombination,[4,5] and defect-related radiative transitions in the QWs.[7,8] The parasitic long-wavelength emission bands strongly influence the electrical and optical properties of GaInN blue LEDs including the subthreshold forward leakage current and the color purity of the emission.[4,5] Therefore, it is critical to understand the origin of parasitic long-wavelength emission bands in GaInN blue LEDs.

In this paper, we report on GaInN blue LEDs that have the major emission band at 445 nm (that is, dominant at typical operating current densities) as well as a cyan emission band at about 480 nm (that is, dominant when the injection current density is very low). The cyan emission band is spatially uniform and can be found in LEDs made by major LED manufacturers, thereby suggesting that the cyan emission band is of a fundamental nature. However, while some LEDs exhibit cyan luminescence (CL), others do not. We denote the LEDs exhibiting cyan luminescence as CL LEDs and the LEDs not exhibiting cyan luminescence as non-cyan-luminescence LEDs (non-CL LEDs). Based on photoluminescence (PL) using resonant optical excitation, we conclude that the cyan emission originates from the active region. Based on electroluminescence (EL) and excitation-density dependent photoluminescence measurements, we identify the cyan emission of the CL LEDs as a radiative transition from the conduction band to an impurity. Based on ionization energy considerations, we identify the impurity as magnesium (Mg) acceptors having diffused into the last-grown quantum well (QW) of the active region.

We also investigate the electrical properties of CL and non-CL GaInN blue LEDs. We find that the subthreshold forward leakage current is higher in the CL LEDs than in the non-CL LEDs. We show that Mg in the active region provides an additional path for carrier transport, which can explain the higher subthreshold forward leakage current found in the CL LEDs.

II. EPITAXIAL GROWTH AND DEVICE FABRICATION

The CL and non-CL LEDs used in this study are GaInN LEDs grown on *c*-plane sapphire substrates by metalorganic vapor-phase epitaxy using the typical organometallic precursor chemistry for the group-III elements and an ammonia precursor for the group-V element. Si and Mg are used as donor and acceptor impurities, respectively. A Si-doped n-type GaN layer precedes the active region of the two types of LEDs (CL LEDs and non-CL LEDs). The active region of the two types of LEDs consists of five 3.0 nm thick undoped GaInN QWs separated by 5 nm thick undoped GaN quantum barriers. The active region is followed by a 30 nm thick heavily Mg doped p-type $Al_{0.15}Ga_{0.85}N$ electron-blocking layer ($N_{Mg} = 8 \times 10^{19}$ cm^{-3}), and a 100 nm p-type GaN layer ($N_{Mg} = 4 \times 10^{19}$ cm^{-3}). After the epitaxy growth, the wafers were fabricated into 1 mm × 0.5 mm LED chips using the standard lithography and dry etching process. Ti/Al and transparent indium tin oxide are employed

[a)]E-mail: shanqf@gmail.com.

 © 2012 American Institute of Physics

as n-contact and p-contact, respectively. The two contacts are located side-by-side on the top surface of the devices.

The CL and non-CL LEDs follow the same growth and fabrication procedures. Since the difference between CL LEDs and non-CL LEDs is apparent from photoluminescence measurements after wafer growth, we can attribute the difference between CL LEDs and non-CL LEDs to small variations, e.g., wafer surface temperature, which occur during epitaxial growth.

III. EXPERIMENTAL RESULTS AND DISCUSSIONS

EL measurements on CL and non-CL LEDs are performed at room temperature. In the EL measurements, the emitted light of a LED is collected using an optical fiber and the spectra are measured by a high-resolution spectrometer. The EL measurement results for a non-CL and a CL GaInN LED are shown in Fig. 1.

Figure 1(a) shows the room-temperature EL spectrum of a non-CL LED at 50 μA. The non-CL LED has only one emission band centered at 440 nm. Figure 1(b) shows the room-temperature EL spectra for a CL LED at a series of different injection currents. Inspection of Fig. 1(b) reveals that at low injection currents, the CL LED exhibits both the blue and the cyan emission band. The EL emission spectra of the CL LED shown in Fig. 1(b) are normalized to the cyan emission peak. When the injection current is below 1 mA, two emission bands are found (445 nm and 480 nm) with the 480 nm cyan emission peak dominating the spectrum. At such low current, we observe, under a microscope, a spatially very uniform cyan emission over the entire chip area. When the injection current is increased from 100 μA to 50 mA, the blue peak of both the CL and non-CL LED undergoes a very small wavelength shift (<1 nm).

In addition to EL measurements, we also perform room-temperature PL measurements on CL and non-CL LEDs. For the PL measurements, we employ resonant optical excitation using an excitation wavelength of 405 nm. The photon energy of the excitation is larger than the bandgap energy of the GaInN QWs, but smaller than the bandgap energy of the GaN quantum barriers, n-type GaN layer, and p-type GaN layer. Thus, only the GaInN QWs are excited (resonant optical excitation) and we assume that most carriers excited in the QWs will recombine in the QWs. Figure 2(a) shows the PL spectrum of a non-CL LED with absorbed excitation density of 0.25 kW/cm^2 (assuming 2% absorption per QW). The non-CL LED has only one emission band centered at 440 nm. Figure 2(b) shows the PL spectra of a CL LED under different excitation densities. Inspection of Fig. 2(b) reveals that the CL LED exhibits both blue and cyan emission under resonant optical excitation. The PL spectra of the CL LED are normalized to the cyan emission peak. Similar to EL, the blue peak of both the CL and non-CL LED undergoes a very small wavelength shift (<1 nm) when increasing the excitation density.

A. Origin of the cyan emission

Since in resonant-excitation PL measurements, only the GaInN QWs are excited, and the emission originates from the QWs, the cyan emission found in the PL measurements, as shown in Fig. 2(b) is concluded to originate from a radiative transition in the GaInN QWs of the active region. Moreover, it is found that the blue and cyan emission bands, found in PL, have peak wavelengths that are identical (or very close) to the peak wavelengths of the same two emission bands found in EL. Therefore, we also attribute the cyan emission found in EL to a radiative transition occurring in the GaInN QWs of the active region.

We next discuss the intensity ratios of the two peaks and how they depend on the excitation density. As the injection current increases in EL measurements of the CL LED, the blue emission increases more rapidly than the cyan emission, so that the blue-to-cyan intensity ratio increases. This EL

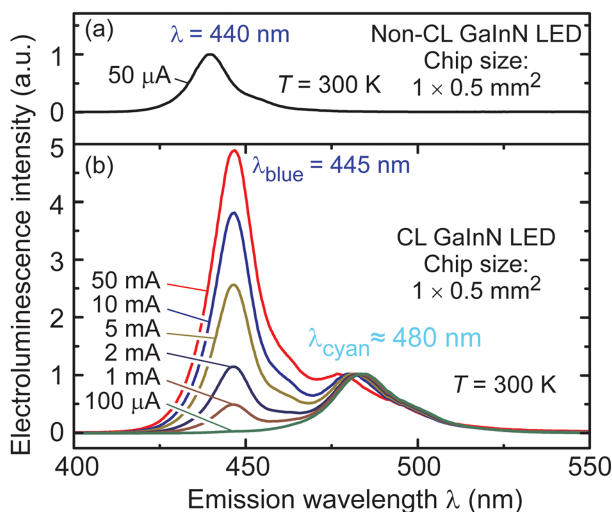

FIG. 1. (a) Normalized room-temperature EL spectrum of the non-CL LED measured at 50 μA. (b) Room-temperature EL spectra of the CL LED at different current levels. The EL spectra of the CL LED are normalized to the cyan emission peak.

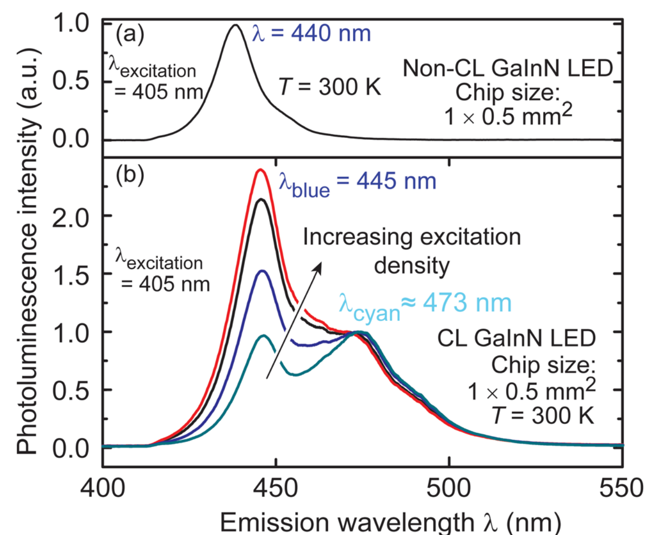

FIG. 2. (a) Normalized room-temperature PL spectrum of non-CL LED with absorbed excitation density of 0.25 kW/cm^2 (assuming 2% absorption per QW). (b) Room-temperature PL spectra of CL LED under different absorbed excitation densities (from low to high): 0.25 kW/cm^2, 0.58 kW/cm^2, 1.30 kW/cm^2, 2.03 kW/cm^2 (assuming 2% absorption per QW). The PL spectra of the CL LED are normalized to the cyan emission peak.

behavior is shown in Fig. 1(b). The same behavior is found in PL: Figure 2(b) shows that as the excitation density increases, the blue-to-cyan intensity ratio increases as well. In other words, by increasing either the injection current or the photo-excitation density, the blue-to-cyan intensity ratio increases. The behavior of the blue and cyan emission, and their intensity ratio, is typical for the free-to-free transitions and free-to-bound transitions, respectively.[9,10] Free-to-free transitions are transitions between bands (conduction and valence band). Free-to-bound transitions are transitions between a band (conduction or valence band) and localized impurity states. We attribute the blue emission band found in EL and PL to near-band-edge free-to-free transitions in the GaInN QWs. We attribute the cyan emission to a free-to-bound transition with participation of a localized impurity state.

Next, we explain why the attribution of the cyan emission to a free-to-bound transition with participation of a localized impurity state is consistent with the measurements. When the carrier concentration in the active region is low, there are more impurity states than free carriers. Therefore, free-to-bound electron-to-impurity transitions are more likely to occur than free-to-free electron-to-hole transitions. Therefore, at low currents, the cyan emission dominates. With increasing injection current or excitation density, due to the limited number of impurity states, the blue emission grows faster than the cyan emission, and therefore, the blue-to-cyan intensity ratio increases. These arguments support our attribution of the cyan luminescence band to a free-to-bound transition.

The photon energy difference between the blue emission (445 nm) and cyan emission (480 nm) is $\Delta\ (h\nu) = h\nu_{\mathrm{blue}} - h\nu_{\mathrm{cyan}} = 203$ meV. This energy difference is very close to the difference in GaN band-edge emission (3.4 eV) and the so-called "3.2 eV emission line" observed in low and moderately Mg-doped p-type GaN.[10–14] The 3.2 eV emission in GaN:Mg has been attributed to radiative transitions from the conduction band to Mg acceptors (e–A^0 transition).[10,12] It has been reported that Mg atoms in the EBL and p-type GaN layer can diffuse into the last-grown quantum barrier layer or even the last-grown QW.[4,15–17] A similar parasitic emission was also observed in GaInN LEDs with the active region intentionally contaminated by Mg.[7] Therefore, we attribute the cyan emission in CL LEDs to radiative transitions from the conduction band to Mg acceptors in the last-grown QW, as illustrated in Fig. 3. Although the CL and non-CL LEDs follow the same growth and fabrication procedures, Mg diffusion may occur due to slight variations of experimental conditions, e.g., the surface temperature and the Mg precursor flow rate during the epitaxy growth of the p-type region of CL LEDs.[15–17]

B. Analysis on current-voltage characteristics

A LED can be modeled as an equivalent electrical circuit consisting of (i) a pn junction diode, (ii) a parallel resistor, (iii) a parasitic diode, and (iv) a series resistor.[18] For applied voltages $V \gg k_B T/e$, the pn junction diode has the current-voltage (I–V) characteristic:[19,20]

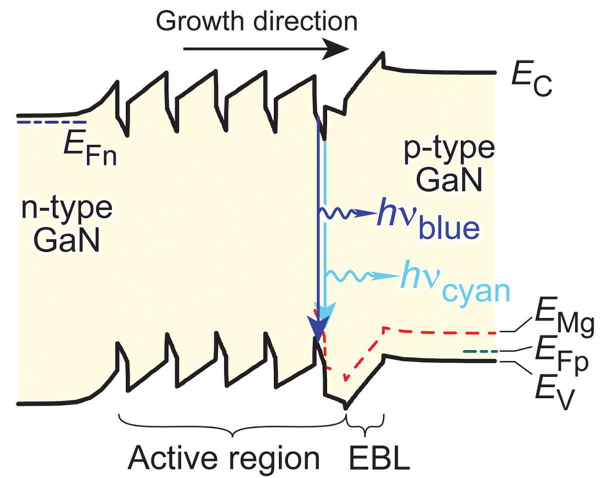

FIG. 3. Schematic band diagram of the CL LED under the forward bias. The cyan emission is due to a transition from the conduction band to a Mg acceptor having diffused into the last-grown QW.

$$I_J = I_1 \exp\left(\frac{e\ V_J}{n_{\mathrm{ideal}}\ k_B\ T}\right), \tag{1}$$

where I_J and V_J are the current and voltage of the pn junction diode, respectively, I_1 is the reverse saturation current, e is the elementary charge, n_{ideal} is the diode-ideality factor, k_B is the Boltzmann constant, and T is the absolute temperature. The parallel resistor represents the surface[21] and bulk leakage current.[3,22] The parasitic diode displays a lower turn-on than the pn junction diode, i.e., a premature turn-on. The current through the parasitic diode could be due to leakage through surface states at the perimeter of the diode chip,[18] the generation-recombination process,[23] or the "diagonal tunneling" of carriers through the band gap.[3] The "diagonal tunneling" is the process where an electron (or a hole) tunnels from the conduction band (or valence band) of n-type GaN (or p-type GaN) to the valence band (or conduction band) of p-type GaN (or n-type GaN) following a staircase route assisted by the intermediate states in the band gap.[3] The I–V characteristic of the parasitic diode can be described by the empirical equation:[3,18,23]

$$I_P = I_2 \exp\left(\frac{e\,V_P}{E_0}\right), \tag{2}$$

where I_P and V_P are the current and voltage of the parasitic diode, respectively; I_2 is the reverse saturation current of the parasitic diode; and E_0 is a characteristic energy. The series resistor represents the metal-to-semiconductor contacts and the bulk resistance of the n-type and p-type materials.[23] Using Eqs. (1) and (2) and considering the parallel resistance and the series resistance, the I–V characteristic of the LED (i.e., pn junction diode plus parasitic diode plus parallel and series resistors, see inset of Fig. 4) can be described by[18,23]

$$I - \frac{V - I\ R_S}{R_P} - I_2 \exp\left[\frac{e\ (V - I\,R_S)}{E_0}\right] = I_1 \exp\left[\frac{e\ (V - I\ R_S)}{n_{\mathrm{ideal}}\ k_B\ T}\right], \tag{3}$$

where R_S and R_P are the series and parallel resistance, respectively.

Figure 4 shows I–V measurements for a CL LED and a non-CL LED with the current plotted using a logarithmic scale. The equivalent electric circuit of the LED is shown in the inset of Fig. 4. At very low forward voltage (below 1.5 V), the pn junction diode is highly resistive.[5] Since $R_P \gg R_S$,[18] the current-voltage characteristic of the LED in the low voltage range is determined by the parallel resistance R_P. The parallel resistance R_P is extracted by a linear fit to the experimental I–V data for applied forward voltage less than 1.5 V. As shown in Fig. 4, the current of the non-CL LED at a voltage lower than 1.5 V is below the measurement limit. Therefore, only the lower limit of the parallel resistance of the non-CL LED can be obtained, i.e., $R_{P,non\text{-}CL} \geq 5 \times 10^{10}$ Ω. When a GaInN LED is forward biased at around 1.5–2.0 V, the I–V curve shows a premature turn-on due to the leakage current through the parasitic diode. According to Eq. (2), the characteristic energy E_0 of the parasitic diode is determined by the slope of ln (I)-versus-V plot in this voltage range.[3,23] When a GaInN LED is forward biased at around 2.0–2.5 V, the space charge region of the pn-junction diode dominates the I–V characteristic.[20] In this region, the ideality factor n_{ideal} of the pn junction diode is determined from the slope of ln (I)-versus-V plot.[19] The series resistance R_s of a LED is obtained by plotting the tangent to the I–V curves on the linear scale at voltages far exceeding turn-on.[18] Using this circuit model and the procedure described, we fit a theoretical I–V characteristic to the experimental I-V characteristic for both the CL LED and non-CL LED. The theoretical fits are shown as the dashed curves in Fig. 4 along with the fitting parameters used. As shown in Fig. 4, the fittings for the CL and non-CL LED are nearly perfect.

Inspection of Fig. 4 reveals that the parallel resistance R_P of the CL LED is smaller than that of the non-CL LED, i.e., $R_{P,CL} \ll R_{P,non\text{-}CL}$. This is a manifestation of the larger forward leakage current. It was proposed that the subthreshold forward leakage current of GaInN based LEDs at the forward voltage less than 1.5 V is mostly composed of defect-assisted tunneling.[2,3,22,24] In this process, electrons tunnel from the conduction band of the n-type side, through localized defect states in the band gap, to hole states in the valence band of the p-type side. In the CL LED, there are more Mg acceptors having diffused into the active region. It is well known that dopants in general and Mg acceptors in particular also cause defect states to occur.[25] Therefore, the Mg acceptors and the defect states associated with the Mg acceptors, particularly those having diffused into the active region, provide an additional path for defect-assisted tunneling. This can explain the much greater subthreshold forward leakage current in the CL LED and the smaller parallel resistance of the CL LED.

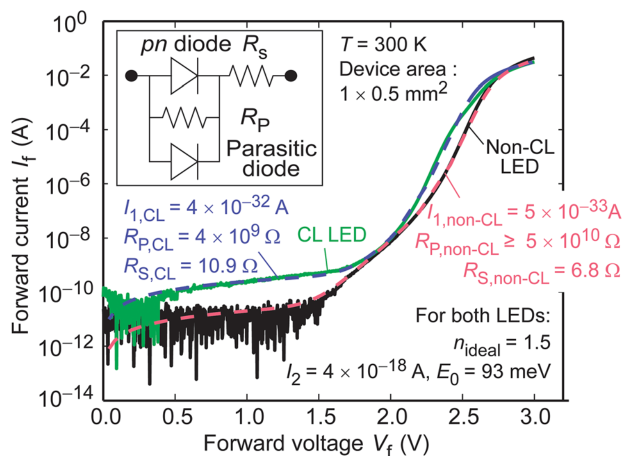

FIG. 4. Forward I–V characteristics of a CL LED (green trace) and a non-CL (black trace) LED. We use the theoretical circuit model shown in the inset and vary the parameters I_1, and I_2 so that the resulting theoretical I–V data (dashed curves) best fit the experimental I–V data (solid curves).

When the applied voltage is between 1.5 V and 2.0 V, the I–V curves display premature turn-on due to the parasitic diode. It is found that the currents of the CL and non-CL LED in this voltage range are very similar. This is consistent with the fact that the fitting parameters of the parasitic diode of the CL and non-CL LED are the same. Therefore, we believe that the Mg atoms diffusing into the active region do not strongly affect I_2 and E_0 of that parasitic diode. It was reported by Lee *et al.*[23] that I_2 and E_0 are strongly influenced by the presence of threading dislocations.

Inspection of Fig. 4 also reveals that the CL LED has a larger reverse saturation current I_1 than the non-CL LED. This is explained by the following: In EL and PL measurements, as shown in Figs. 1 and 2, respectively, the peak wavelength for the band-edge emission, i.e., the blue emission, of the CL LED (445 nm) is a little longer than that of the non-CL LED (440 nm). These EL and PL results indicate that the GaInN QWs of the CL LED have smaller bandgap energy than the non-CL LED. The reverse saturation current follows the equation: $I_1 \propto \exp(-E_g/k_BT)$.[18] Therefore, the CL LED has a larger reverse saturation current I_1.

IV. SUMMARY

In summary, we analyze the optical and electrical properties of two types of GaInN blue LEDs: Both types of LEDs emit blue luminescence; however, one type of LED, the CL LED, emits a cyan luminescence band (480 nm) at very low injection currents, whereas the other type of LED, the non-CL LED, does not emit such a cyan emission band. PL measurements on CL LEDs, using resonant optical excitation, show both the blue and cyan emission bands, indicating that the cyan emission is from a quantum well of the active region. The blue and cyan emission bands found in PL have peak wavelengths very close to the peak wavelengths of the same two emission bands found in EL; this indicates that the cyan emission in EL also originates from the active region. The blue-to-cyan intensity ratio increases with increasing injection or photo-excitation of carriers in the GaInN QWs; this indicates that the cyan emission is due to a transition from the conduction band to an impurity. Based on the ionization energy considerations, this impurity is identified as Mg acceptors having diffused into the last-grown quantum well of the active region.

The electrical properties of the CL and non-CL GaInN LED are investigated. The measured I–V curves for both the

CL and non-CL LED are excellently fitted by theoretical curves generated by the equivalent electric circuit model consisting of a pn junction, a parallel resistor, a parasitic diode, and a series resistor. The fitting reveals that the parallel resistance of the CL LED is smaller than that of the non-CL LED. In CL LEDs, the Mg acceptors and defect states associated with the Mg acceptors in the active region provide an additional path for the defect-assisted tunneling process when the LED is under low forward bias. This explains the measured higher subthreshold forward leakage current and the smaller parallel resistance of the CL LED.

ACKNOWLEDGMENTS

The authors gratefully acknowledge support by Samsung Electronics Co. Sandia National Laboratories, the US National Science Foundation, the Korean Ministry of Knowledge Economy, the Korea Institute for Advancement of Technology, and Magnolia Optical Technologies, Inc. Authors J.C. and E.F.S. were supported by Sandia's Solid-State Lighting Sciences Center, an Energy Frontier Research Center funded by the U. S. Department of Energy, Office of Basic Energy Sciences.

[1]Q. Shan, D. S. Meyaard, Q. Dai, J. Cho, E. F. Schubert, J. K. Son, and C. Sone, Appl. Phys. Lett. **99**, 253506 (2011).
[2]X. A. Cao, S. F. LeBoeuf, K. H. Kim, P. M. Sandvik, E. B. Stokes, A. Ebong, D. Walker, J. Kretchmer, J. Y. Lin, and H. X. Jiang, Solid-State Electron. **46**, 2291 (2002).
[3]D. Yan, H. Lu, D. Chen, R. Zhang, and Y. Zheng, Appl. Phys. Lett. **96**, 083504 (2010).
[4]A. Mao, J. Cho, Q. Dai, E. F. Schubert, J. K. Son, and Y. Park, Appl. Phys. Lett. **98**, 023503 (2011).
[5]V. E. Kudryashov and A. É. Yunovich, J. Exp. Theor. Phys. **97**, 1015 (2003).
[6]B. Leung, Y. Zhang, C. D. Yerino, J. Han, Q. Sun, Z. Chen, S. Lester, K.-Y. Liao, and Y.-L. Li, Semicond. Sci. Technol. **27**, 024016 (2012).
[7]M. Schillgalies, A. Laubsch, St. Lutgen, A. Avramescu, G. Brüderl, D. Queren, and U. Strauss, Phys. Status Solidi C **5**, 2192 (2008).
[8]F. Scholz, V. Härle, F. Steuber, A. Sohmer, H. Bolay, V. Syganov, A. Dörnen, J.-S. Im, A. Hangleiter, J. Y. Duboz, P. Galtier, E. Rosencher, O. Ambacher, D. Brunner, and H. Lakner, Mater. Res. Soc. Symp. Proc. **449**, 3 (1997).
[9]W. Grieshaber, E. F. Schubert, I. D. Goepfert, R. F. Karlicek, Jr., M.-J. Schurman, and C. Tran, J. Appl. Phys. **80**, 4615 (1996).
[10]E. Oh, H. Park, and Y. Park, Appl. Phys. Lett. **72**, 70 (1998).
[11]H. Amano, M. Kitoh, K. Hiramatsu, and I. Akasaki, J. Electrochem. Soc. **137**, 1639 (1990).
[12]M. A. Reshchikov, G.-C. Yi, and B. W. Wessels, Phys. Rev. B **59**, 13176 (1999).
[13]U. Kaufmann, M. Kunzer, M. Maier, H. Obloh, A. Ramakrishnan, B. Santic, and P. Schlotter, Appl. Phys. Lett. **72**, 1326 (1998).
[14]M. A. Reshchikov and H. Morkoç, J. Appl. Phys. **97**, 061301 (2005).
[15]K. Köhler, T. Stephan, A. Perona, J. Wiegert, M. Maier, M. Kunzer, and J. Wagner, J. Appl. Phys. **97**, 104914 (2005).
[16]S.-N. Lee, J. K. Son, H. S. Paek, Y. J. Sung, K. S. Kim, H. K. Kim, H. Kim, T. Sakong, Y. Park, K. H. Ha, and O. H. Nam, Appl. Phys. Lett. **93**, 091109 (2008).
[17]K. Köhler, R. Gutt, S. Müller, J. Wiegert, H. P. Menner, L. Kirste, H. Protzmann, and M. Heukenm, J. Cryst. Growth **321**, 15 (2008).
[18]E. F. Schubert, *Light-Emitting Diodes*, 2nd ed. (Cambridge University Press, Cambridge, 2006).
[19]J. M. Shah, Y.-L. Li, Th. Gessmann, and E. F. Schubert, J. Appl. Phys. **94**, 2627 (2003).
[20]D. Zhu, J. Xu, A. N. Noemaun, J. K. Kim, E. F. Schubert, M. H. Crawford, and D. D. Koleske, Appl. Phys. Lett. **94**, 081113 (2009).
[21]H. Kim, J. Cho, Y. Park, and T.-Y. Seong, Appl. Phys. Lett. **92**, 092115 (2008).
[22]L. Hirsch and A. S. Barrière, J. Appl. Phys. **94**, 5014 (2003).
[23]S. W. Lee, D. C. Oh, H. Goto, J. S. Ha, H. J. Lee, T. Hanada, M. W. Cho, T. Yao, S. K. Hong, H. Y. Lee, S. R. Cho, J. W. Choi, J. H. Choi, J. H. Jang, J. E. Shin, and J. S. Lee, Appl. Phys. Lett. **89**, 132117 (2006).
[24]C. L. Reynolds, Jr. and A. Patel, J. Appl. Phys. **103**, 086102 (2008).
[25]R. L. Longini and R. F. Greene, Phys. Rev. **102**, 992 (1956).